Writing Assignment

0 Layman's Summary

Our vascular system consists of all the vessels in our body, from the smallest microvessels and capillaries to the bigger veins and arteries. Their main responsibility is the transport of blood and, therefore, the endothelial cells that line the inside of our vessels are always in direct contact with our blood. These endothelial cells are able to sense the flow of blood, which is an important aspect of their overall function and vascular health. For example, when the blood does not flow through the vessels normally it can lead to disease, such as atherosclerosis. The process by which cells are able to sense and respond to such mechanical stimuli, such as pressure, flow and stiffness, is known as mechanotransduction. At present, we do not fully understand the mechanisms through which this works, but if we did it could eventually lead to new treatment options or drug development. Therefore, there is a lot of ongoing work trying to unravel the underlying mechanisms in mechanotransduction.

Currently, a popular method to do this research is by using microfluidic devices. These are devices with microscopic channels that, when seeded with endothelial cells, replicate the microvasculature in our body. They are useful because they provide a realistic three-dimensional vessel structure to the cells, because they facilitate easy application of mechanical stimuli like flow and, lastly, because their small size reduces production time and reagent costs. Moreover, should these microfluidic vessel models at some point in the future become highly similar to our real vessels, they can help to bridge the gap from animal to human testing in clinical trials, and perhaps replace animal testing altogether. Overall, they are a more efficient method to recreate and study mechanotransduction of endothelial cells than traditional methods (petri-dish cultures).

This report reviews the methods used in studies that investigate mechanotransduction using microfluidic endothelial models. First, it discusses methods used to confirm if new models accurately replicate the mechanical stimuli, which involves computational models and specialized equipment. Then, similarly, it discusses methods used to confirm if new models form vessels that match the study's expectation, which involves different microscopy techniques and image analysis. Lastly, methods are discussed that are used to investigate mechanotransduction processes in microfluidic endothelial models, which involves a variety of biochemical analysis techniques. To conclude, drawbacks of current models are discussed, such as low protein contents for quantitative analysis, and a shift towards more model improvement is recommended.

Characterization methods of mechanobiology in novel microfluidic endothelial models.

Tom van de Kemp

The vascular system comprises a vast network of arteries, veins and microvessels lined with endothelial cells (ECs), which help maintain vascular homeostasis. While we understand that the ECs that arise from these tissues have distinct phenotypes and functions, we do not fully understand the role of their microenvironment, specifically how they interpret mechanical stimuli, such as hemodynamic flow, shear stress, stretching and stiffness. By employing microfluidic endothelial models, we attempt to effectively recreate this microenvironment so that we can unravel the associated mechanobiological pathways, in order to inform future studies in human disease and drug design. The current state-of-the-art has already been extensively reviewed, however characterization methods are less often discussed. Therefore, this review aims to provide a framework for characterization of microfluidic endothelial models by discussing methods used for model validation, as well as investigation into mechanobiological pathways. Ultimately, as future reference and outlook, recurring patterns and commonly encountered problems from the recent literature are also addressed.

1 Introduction

The vascular system experiences a variety of physical stresses as a result of its primary function, the transport of blood. Endothelial cells (ECs), which line the inside of the vessel walls, translate these mechanical cues to biochemical signals by mechanotransduction and have an important regulatory role in maintaining homeostasis [1]. Accordingly, an abnormal mechanical microenvironment is a contributing factor in disease, such as in atherosclerosis [2] and cancer [3], which are primary causes of death worldwide [4]. Therefore, it is highly valuable to investigate the fundamentals of endothelial mechanotransduction, as it can help us find ways to prevent progression into pathological phenotypes. However, until recently, its importance was not reflected in the research models, because traditional two-dimensional (2D) cell-culture methods fail to successfully recreate the mechanical microenvironment, especially in terms of geometry and mechanical stimuli [5]. This emphasizes a need for more physiologically-relevant models.

In normal physiology, the mechanical stimuli endured by ECs range from different types of fluid flow, to interactions with their extracellular matrix (ECM) (*Figure 1*). Firstly, the ECs directly experience shear stress (SS) from blood flow in the lumen. Secondly, different flow types (interstitial flow (IF), transvascular flow (TVF) and bifurcated fluid flow (BFF)) may also exert shear forces on ECs but in different directions. Additionally, ECs may experience cyclic strain due to stretching of the vessels, in response to pulsatile blood flow. Lastly, ECM stiffness may also vary depending on its local composition [6]. In comparison, diseases may be characterized by pathological dynamic phenotypes (*e.g.* atherosclerosis; low SS, disturbed

flow (DF), high stiffness) [2, 7]. Through mechanotransduction, ECs are able to sense all these stimuli together and their known mechanobiological pathways have been previously reviewed [1, 8]. Therefore, a good biomimetic endothelial model should attempt to simulate all relevant elements.

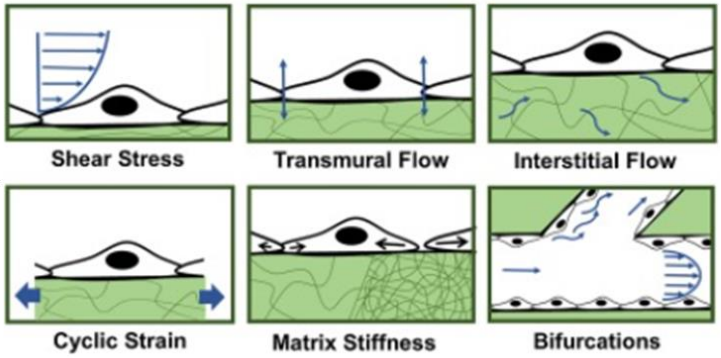

Figure 1: Overview of the mechanical stimuli and flow types discussed in this review. Blue arrows represent direction of fluid flow, black arrows show direction of contractile forces (here, cyclic strain) in endothelial cells (ECs). The green area and its crinkly lines represent extracellular matrix (ECM) and basement membrane components. Adapted from [6].

Due to progress in microfluidics and three-dimensional (3D) cell-culturing methods, microfluidic devices (MFDs) have become a popular platform for modelling a physiologically-relevant endothelial microenvironment. Firstly, MFDs have a major advantage simply because of their small scale, which allows for the use of less reagent volumes, faster device-fabrication time and also the possibility of integrated analysis methods. Secondly, more specifically related to the endothelial model itself, MFDs allow for strong replication of the microenvironment on a number of levels. For example, the vessel geometry can be easily replicated because hydrogel channels can accommodate the formation of 3D cell tubes. Similarly, relevant ECM with tuneable stiffness can also be simulated through the use of certain hydrogels with crosslinking capacity [9]. Additionally, different flow profiles and SS levels can be effectively recreated through the perfusion and structure of MFDs (Figure 2) [10]. Examples of microfluidic endothelial models with a dynamic biomimetic microenvironment have already been extensively reviewed elsewhere [11, 12]. However, while the development of such systems is frequently reported, their validation and characterization methods have never been reviewed.

Therefore, here, the characterization methods of endothelial microfluidic models and of associated mechanobiological pathways are reviewed from the recent literature. This review will firstly give an overview of, and elaborate on, methods used to evaluate mechanical stimuli and biological parameters to validate microfluidic endothelial models. Then, established methods and innovative approaches by which the mechanobiology is characterized are discussed. Ultimately, as future reference, this review aims to provide a framework for characterization methods and recommendations based on observed patterns and problems.

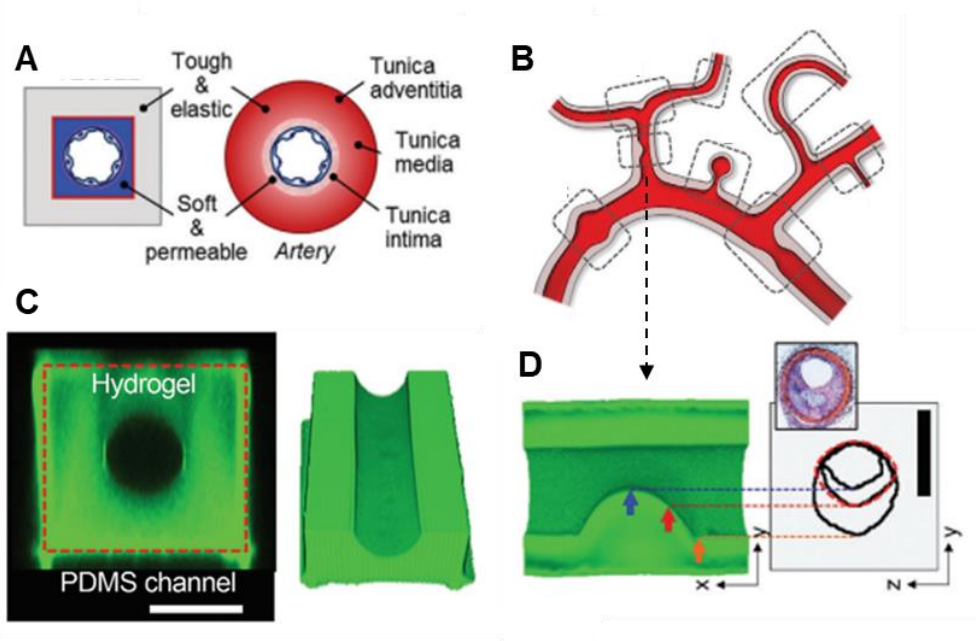

Figure 2: Recreation of a vessel in a microfluidic device. A) Schematic comparison between a microfluidic model and healthy artery. B) Schematic representation of different types of luminal shapes that can be achieved in a microfluidic channel. C) Confocal microscope images of the cross-section (left) and a 3D-representation (right) of the lumen and hydrogel-PDMS interface in a microfluidic device. D) Confocal microscope image of non-axisymmetric lumen (left) and its cross-section (right), which mimics the coronary artery with an atherosclerotic plaque seen in the histological cross-section in the inset. Adapted from [10].

2 Model Validation: Mechanical Stimuli

Prior to evaluating the EC response to any type of stimulus supplied by the model system, there should be certainty that the system can accurately create the desired conditions. This comes down to model validation, which is an essential aspect of the development process. In the literature, different methods are used to evaluate if the mechanical stimuli are accurately applied in the microfluidic models.

Because the primary function of the vasculature is fluid transport, it makes sense that shear stress and flow type are most commonly studied. Moreover, it is exactly the ability to precisely apply different flows in microfluidic devices that sets them apart from other models. For example, a study on EC response to only stiffness, would not necessitate the use of microfluidics. Therefore, since this review deals with microfluidic endothelial models, even the studies that focus on stiffness or cyclic strain also evaluate their application of flow. This is illustrated in Figure 3, which gives an overview of the distribution of the number of studies that evaluate mechanical stimuli in the reviewed literature (Table 1+2) and their corresponding values *in vivo*.

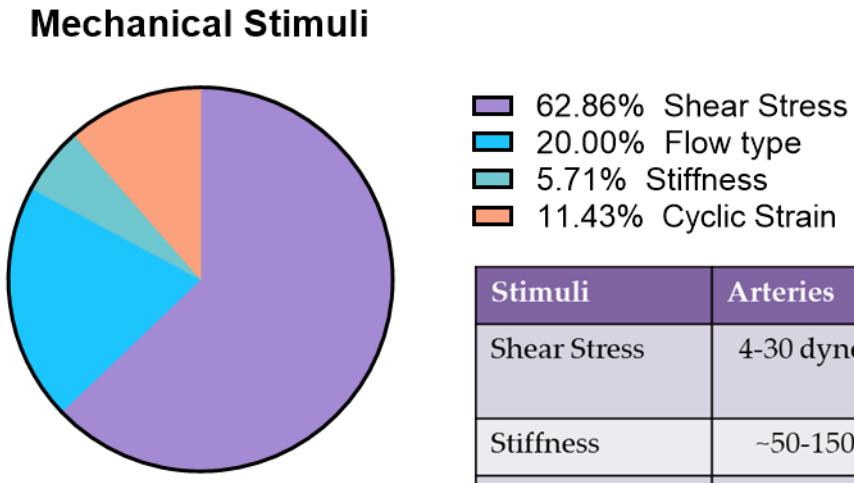

Stimuli	Arteries	Veins
Shear Stress	4-30 dyne/cm^2	1-4 dyne/cm^2
Stiffness	~50-150 kPa	~3-50 kPa
Cyclic Strain	~7-11%	<10%

Figure 3: Overview of reported mechanical stimuli in all the reviewed literature (chart) and of the values of mechanical stimuli in vivo (table) adapted from [6, 13].

2.1 Shear Stress and Flow Types

Often, computational models are utilized to identify the magnitude and direction of the flows inside the channels of the microfluidic device (Figure 4A). Fluid flows are most commonly modelled by employing the Navier-Stokes equations *(1)*, a system of partial differential equations that allow for the simulation of the flow situation in the microfluidic device [14].

$$\rho[\partial_t v + (v \cdot \nabla)v] = -\nabla p + \eta\nabla^2 v + \beta\eta\nabla(\nabla \cdot v) + \rho g \quad (1)$$

These arise from application of Newton's second law of motion to fluids, where the left hand side incorporates mass (ρ; fluid density) and acceleration ($[\partial_t v + (v \cdot \nabla)v]$; change in velocity over time plus speed and direction of fluid), while the right hand side is a total sum of the forces acting on the fluid (*i.e.* pressure gradient, $[-\nabla p]$; viscous term, $[\eta\nabla^2 v + \beta\eta\nabla(\nabla \cdot v)]$; gravity, $[\rho g]$). However, for these underlying equations to be valid, it is essential that some fundamental assumptions are satisfied [15], namely:

1) Newtonian framework; concerns the separate conservation of mass and energy and excludes any relativistic effects because none of the velocity components in the model approach the speed of light. Additionally, all the involved fluids are assumed Newtonian and thus maintain their original viscosity under shear force.
2) Continuum modelling; implies that because matter is significantly larger than the inter-atomic distance between its atoms, it can be modelled as a continuous object. This allows us to describe its properties with a system of differential equations. For example, by applying conservation of mass from assumption 1), the continuity equation can be derived [16]:

$$\partial_t \rho = -\nabla \cdot (\rho v) \quad (2)$$

For a fluid, this states that the rate of mass decrease over time $[-\nabla \cdot (\rho v)]$ out of an element must be equal to the rate of mass decrease over time out of the total volume $[\partial_t \rho]$. Simply put, since mass cannot simply appear or disappear, the total mass can only change when volume is lost through flow.
3) Thermodynamic (quasi-)equilibrium; ensures that macroscopic quantities, such as temperature, volume and mass, have enough time to adjust to the changing environment and ties in with (1), *i.e.* conservation of energy. The commonly applied no-slip boundary condition, resulting in zero velocity at the channel walls, also arises from this assumption.

Then, depending on the specific situations in the microfluidic device, additional assumptions and conditions may be applied. For example, in most microfluidic channels the assumption of incompressible flow is also valid because the flow velocity is significantly smaller than the speed of sound. This means that no change of volume will occur and, therefore, the continuity equation is simplified to (2.1) [16]. As a result, this also eliminates part of the viscous term $[\beta\eta\nabla(\nabla \cdot v)]$ in the Navier-Stokes equation (3):

$$\nabla \cdot v = 0 \quad (2.1)$$

$$\rho[\partial_t v + (v \cdot \nabla)v] = -\nabla p + \eta\nabla^2 v + \rho g \quad (3)$$

Moreover, the geometry of the channel (*e.g.* rectangular, circular, parallel-plate, etc.) should also be taken into account. Ultimately, the solutions to the Navier-Stokes equations for the given conditions of the microfluidic channel give the flow velocity and profile (*e.g.* Poiseuille flow, Hele-Shaw flow, inviscid flow, *etc.*) and facilitate the determination of other parameters, such as Reynolds number (Re), flow rate (Q) and eventually wall shear stress (τ_{wss}) [16].

Computational modelling can be an effective tool to evaluate the flows inside a microfluidic model, but it is essential that these are measured and validated in the live model as well. Oftentimes, the flow rate is measured through particle image velocimetry (PIV), which involves the loading of particles (*e.g.* cells, fluorescent beads, etc.) into the microfluidic device and imaging their trajectory (Figure 4C). Since the frame rate of the recording and dimensions of the microfluidic device are known, the flow velocity and flow rate may be easily computed using an image analysis software [17-19]. Alternatively, the flow rate is occasionally determined by measuring total fluid displacement at the end of the experiment [20]. Lastly, it is also possible to determine flow rate in real-time by employing a flow sensor (*e.g.* Sensirion, SLI-1000) [17].

2.2 Stiffness

In microfluidic models, stiffness is a difficult quantity to directly measure because it generally requires some form of contact and probing, which may result in destruction of the sample. Additionally, the overall structure of the microfluidic device may also hinder access [10]. Fortunately, since in general, stiffness is a passive material property, it is most commonly determined externally, in a separate sample or film. The simplest method, involves the use of a testing system able to generate the raw data for a stress vs. strain graph. Stiffness is then computed as the slope of the linear region of the curve [21, 22]. Another option, requires the use of atomic force microscopy (AFM). In AFM, the tip of a flexible cantilever, which behaves like a spring, probes a sample by pushing into it, this results in bending of the cantilever as it interacts with a force from the sample, which is recorded together with the indentation depth. Then, a curve representing force (F) vs. indentation depth (x) is fit, from which the stiffness (k) can be simply computed by applying Hooke's law [10, 23]:

$$\mathrm{F} = -k \cdot x \quad (4)$$

The above two methods may also be used in combination [22]. Notably, while stiffness is normally regarded as a passive material property, Yu *et al.* recently developed a microfluidic model with dynamically tuneable stiffness [10].

2.3 Cyclic Strain

Strain may refer to any type of deformation but, when discussing the vascular system, this mainly involves circumferential stretch of the vessel wall in response to blood flow. When stretching of the vessel walls occurs, this deformation can be imaged and then, by employing an image analysis software, the strain can be easily measured [24, 25]. However, interestingly, a novel, microfluidic model with an integrated, stretchable electrochemical sensor was reported by Jin *et al.* [25]. This innovation allows for direct, real-time analysis of the circumferential stretch experienced by the vascular model, without the need for additional imaging and computation.

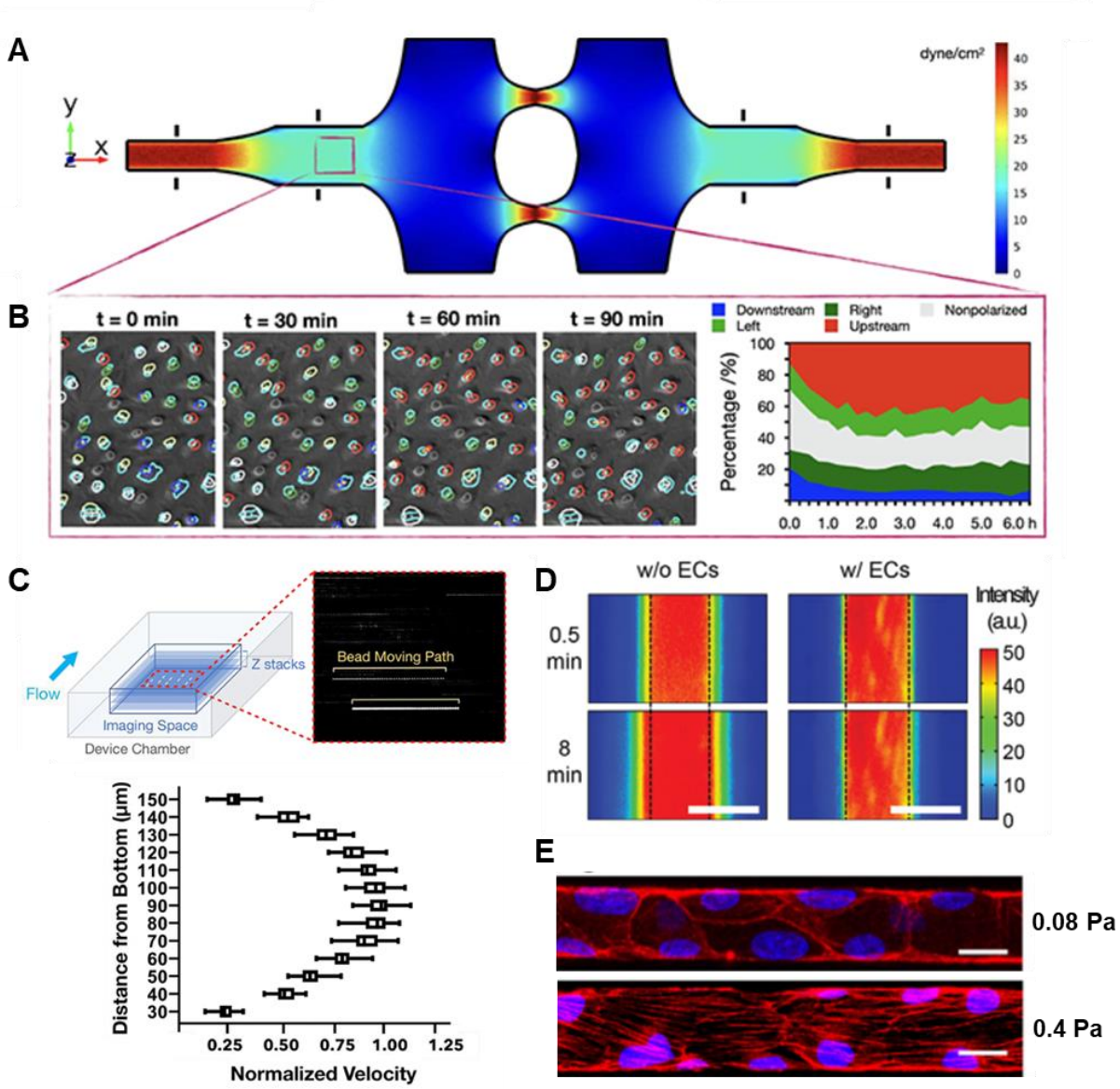

Figure 4: Characterization methods of microfluidic endothelial models. A) Shear Stress (SS) levels in different regions of the microfluidic device (MFD) determined from Navier-Stokes equations. B) Image analysis of nucleus-Golgi orientation in response to SS over time inside region of the MFD. C) Evaluation of flow velocity and profile through particle image velocimetry (PIV), A+B+C adapted from [18]. D) Fluorescence heatmaps after perfusion of FITC-Dextran 40 kDa into the lumen, for assessing vessel permeability without ECs (left) and with ECs (right) (scale bar = 100 µm), adapted from [10]. E) HUVECs stained for nuclei (DAPI, blue) and cytoskeleton (F-actin, red) lining the walls of a microchannel, show more cell elongation and stress fiber alignment after 96-hour-exposure of low SS flow (top) and high SS flow (bottom) (scale bar = 20 µm), adapted from [26].

3 Model Validation: Biology

Once the mechanical conditions of the model are validated, it is ready for perfusion with ECs to allow for monolayer or vessel formation. Then, again, the model should be validated to assess whether the formed vessels resemble the desired vessel physiology. Fortunately, the vessel characteristics and EC phenotypes associated with either healthy or diseased physiologies are established knowledge and therefore, a number of parameters are frequently used to assess whether novel endothelial models are functioning according to expectation. The most commonly evaluated parameters used for model validation in the reviewed literature (Table 1) are described below in Figure 5.

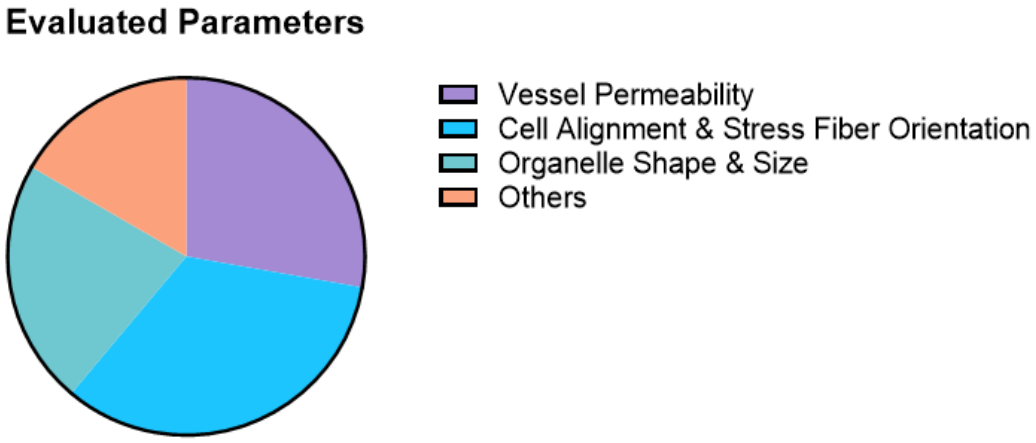

Figure 5: Overview of the evaluated physical parameters in the reviewed literature (Table 1).

3.1 Vessel Permeability

Transport is the main purpose of the vascular system, most importantly of oxygen to ensure sufficient oxygenation of tissues but also of nutrients, waste products and immune cells. Therefore, it is essential that blood vessels are sufficiently permeable, to facilitate an efficient exchange between tissue and circulation [27]. In the healthy vasculature, molecules up to 40 kDa are able to freely diffuse through the mature vessel walls, whereas larger molecules are retained. In disease, however, even molecules of up to 2000 kDa may extravasate from the vasculature. Moreover, aside from the molecular size, the extravasation rate may also depend on molecular shape, charge and hydrophilicity. Lastly, the vascular permeability is also affected by the composition of cell types in the vessel wall [27, 28]. Because it is such a defining property of the vasculature, it is also a highly useful parameter to assess the integrity of new endothelial models.

The standard method for evaluating vessel permeability is by perfusion with a fluorescently-labeled model-macromolecule. Most commonly, this is done with dextran (40 kDa) because of its flexible molecular size, which can be between 500 Da - 23 MDa depending on the length of its polysaccharide chain [29]. To evaluate vessel permeability, the vessel is perfused with the fluorescently-labeled dextran, after which its permeation into the hydrogel surrounding the vessel is observed by fluorescence microscopy. Subsequently, the permeability may be analyzed by employing an image analysis software and computing the relative fluorescence inside a region of interest (ROI) (Figure 4D) [10, 17, 21, 30, 31]. By a similar approach, extravasation of different fluorescently labeled cells through the vessel wall can also be monitored [17, 21, 32], grouped in 'Others' in Figure 5.

3.2 Cell Alignment & Stress Fiber Orientation

It has long been known that as a result of physiological SS-exposure, ECs elongate and align themselves parallel to the flow direction [33]. The mechanosensing of SS, leads to the formation of stress-fibers, composed of actin filaments, that span the entire cell body. These stress fibers then provide stability to the cell by aligning to the SS-direction and contribute to the final elongated cell shape. This is commonly referred to as the atheroprotective phenotype, because random cellular shape and orientation is strongly associated with disfunction and pathological situations, such as atherosclerosis [34]. Therefore, this reorganization of the cytoskeleton in response to SS is a valuable indicator of a functional endothelial model and is often used as parameter for validation.

The visualization of the cytoskeleton, specifically of polymerized actin filaments, is the most straightforward method to evaluate the elongation of ECs and orientation of their stress fibers. Overall, immunocytochemistry is the established laboratory technique for qualitative analysis of proteins in cells by visualization and, therefore, also predominantly applied for this purpose [24, 26, 35-37]. The standard approach involves conjugation of the protein of interest with a fluorescently tagged antibody, or different type of target-binding protein, and imaging with fluorescence microscopy. For the cytoskeleton, fluorescently-labeled phalloidin is often employed because of its high binding affinity for filamentous actin and ability to prevent the dissociation of the actin subunits at both ends, resulting in stabilization of the actin filaments [38]. Then, depending on which type of fluorescent dye is conjugated, the appropriate excitation and emission wavelength should be selected for visualization of the cytoskeleton (Figure 4E) [39]. Finally, the orientation of the stress fibers can be determined by employing an image analysis software.

3.3 Organelle Shape & Size

Aside from alignment in the direction of the flow, ECs are observed to polarize as well in response to experiencing shear flow. In this polarization, the upstream side of the EC retains the Golgi apparatus and centrosomes, while the nucleus is relocated to the downstream side of the cell due to hydrodynamic drag [40]. Additionally, their respective sizes are generally observed to be smaller and less circular. Therefore, the polarization of ECs in response to flow SS, which is characterized by organelle location, size and shape, is also occasionally used to validate a novel endothelial model [18, 35, 36].

Similar to in the previous subsection, these parameters are most efficiently evaluated through visualization of the nucleus and Golgi apparatus by immunocytochemistry and subsequent image analysis. For the nucleus, either Hoechst [18] or DAPI staining [35, 36] (Figure 4E) can be applied for visualization, as they both bind double stranded DNA. For the Golgi apparatus, the use of an antibody stain is a suitable method [18, 41]. Dedicated image analysis methods may then be employed to acquire data on cell polarization and organelle shape and size (Figure 4B) [18].

Table 1: Validation of microfluidic endothelial models (2017-).

Cell type(s)	Stimulus analysed				Evaluated parameters	Results	Ref.
	Shear Stress	Flow types	Stiffness	Cyclic strain			
Human brain-derived microvascular ECs	✓				• Vessel permeability • Cell alignment	• Live, high-resolution imaging of lumen and surrounding collagen matrix. • ECs formed a functional barrier. • SS; ECs aligned in flow direction.	[31]
HCAECs	✓		✓	✓	• Vessel permeability • Cell alignment	• Low SS; ↑ vessel permeability and ↓ NO-production. • ↑ ECM stiffness; ↑ vessel permeability. • ↓ Cyclic strain; ↑ vessel permeability.	[10]
HUVECS Human lung-fibroblasts monocytes	✓		✓		• Vessel permeability • Stress fibre orientation • Extravasation distance	• Stress fibers aligned in flow direction. • SS; ↑ monocyte adhesion but ↓ monocyte extravasation. • ↑ stiffness; ↓ barrier integrity and ↑ extravasation.	[21]
HAECs	✓	✓			• Stress fibre orientation • Nucleus shape/size	• SS; HAECs align parallel to flow direction. DF; align perpendicular. Static; randomly. • DF; ↑ nucleus circularity but ↓ nuclear size.	[35]
HUVECs	✓			✓	• Monocyte adhesion	• Low SS; ↑ ICAM-1 expression and ↑ monocyte adhesion.	[19]

HAECs	✓	✓			• Stress fibre orientation • Nucleus shape/size	• High SS; actin filaments align parallel to flow direction. Low SS; perpendicular. DF/static; randomly. • DF; ↑ nucleus circularity but ↓ nuclear size. • High SS; ↑ nuclear localization of β-catenin. Low SS + DF; ↑ nuclear localization of β-catenin.	[36]
HUVECs	✓				• Nucleus shape/size • Golgi shape/size	• After SS-exposure (2 dyne/cm^2, 3 hours), HUVECs adopt upstream orientation (nucleus to Golgi). • Similar SS-exposure also ↑ nucleus-Golgi distance.	[18]
HUVECs	✓				• Stress fibre orientation	• SS; actin fibers align along the flow direction. • SS (5-fold reduction, 1h); actin cytoskeleton reorganization = disrupted stress fibers + actin redistribution to peripheral band.	[26]
HUVECs Osteocytes Breast cancer cells	✓				• Extravasation distance • Vessel permeability	• Presence of osteocytes ↑ breast cancer cell extravasation in the static condition. • Mechanical stimulation of osteocytes inhibits extravasation.	[17]
HUVECs Monocytes	✓				• Extravasation distance • Vessel permeability	• High-resolution, time-lapse confocal microscopy of extravasation. • Presence of monocytes ↓ cancer cell extravasation.	[32]
HUVECs	✓			✓	• Cell alignment	• Incorporated, stretchable electrochemical sensor in MFD. • Circumferential stretch (> 10%) resulted in EC alignment along the channel.	[25]

4 Characterization of Mechanobiology

Then, when all essential aspects of the endothelial model are validated, it may finally be used for the purpose of investigating the underlying mechanobiological pathways. This is also where it becomes more important to also consider the other features of the model, such as the used EC types and its complexity, specifically their effects on its characterization.

For example, HUVECs are most commonly used because of their high availability, ease of use and abundance in the published literature [42]. However, they are not necessarily representative of each endothelial environment and, while the difference between mechanical stimuli experienced by ECs *in vivo* (*e.g.* arteries *vs.* veins; Figure 3) are discussed during model validation, the associated differential expression of specific EC markers should also be kept in mind while analyzing mechanobiology [43]. Moreover, the complexity of the model also affects its characterization. For visualization especially, the staining and imaging process of a 2D monolayer in a parallel-plate flow chamber is significantly less tedious than a 3D vessel structure in a hydrogel, which requires more sophisticated methods [31, 44]. Furthermore, incorporation of more than one cell type also adds to the complexity. Therefore, identification of cell-specific proteins helps to easily differentiate between multiple cell types in co-culture models [24, 45]. An overview of these features is given in Figure 6, along with an overview of the division between mechanosensing, and signal transducing components of investigated mechanobiological pathways in the other reviewed literature (Table 2), which is further discussed below.

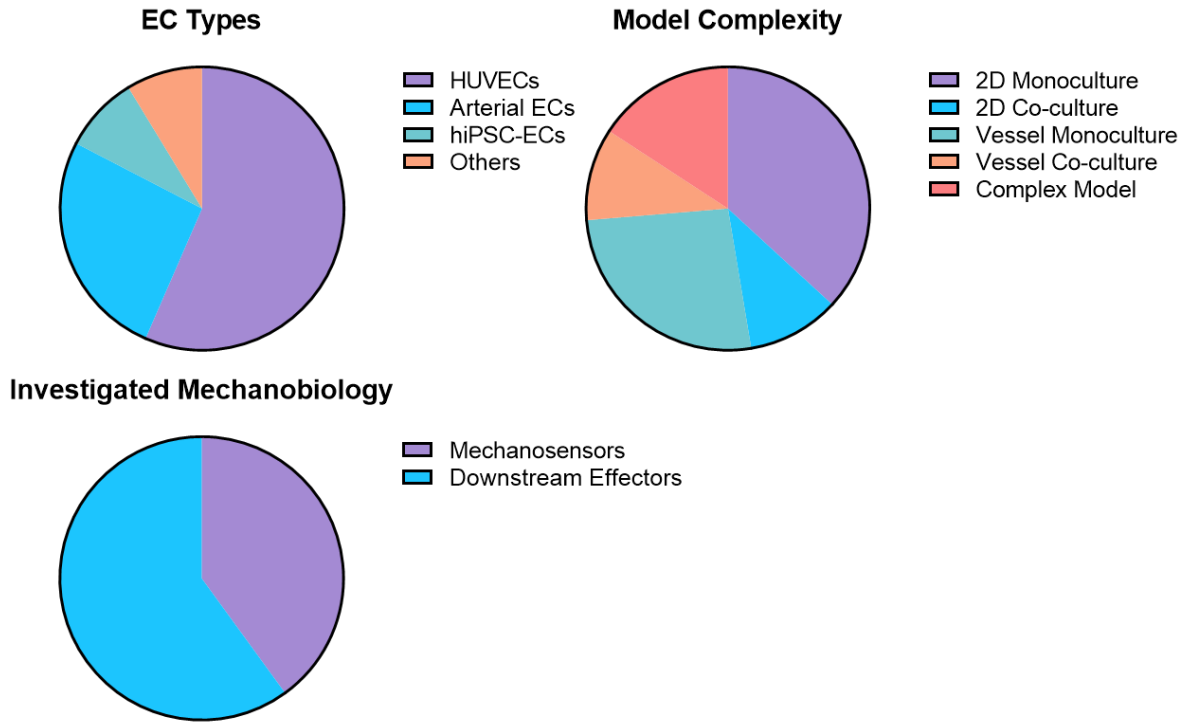

Figure 6: Overview of the used EC types, overall complexity of the models and division between mechanosensing, and signal transducing components of investigated mechanobiological pathways in the reviewed literature (Table 2).

4.1 Mechanosensors & Downstream Effectors

All the reviewed literature, which applied microfluidic endothelial models for the investigation of mechanobiological pathways, identified the mechanosensing components (*e.g.*

integrins, PECAM-1, VE-cadherin, TKRs, ion channels, caveolae, membrane lipids, the glycocalyx and GPCRs) and related downstream effectors under specific mechanical conditions. Overall, more downstream effectors than mechanosensors were reported, which makes sense because more downstream effectors exist than mechanosensors. All these downstream effectors can also work as signal transducers for different mechanosensors, in related pathways and in response to different mechanical stimuli, creating a complex system [8]. To illustrate, an overview of known components in the signaling pathway in response to SS in ECs is shown below in Figure 7. The respective role of each component can be unraveled by employing a combination of analytical techniques, such as qualitative and quantitative determination of protein expression, their localization in the cell, as well as targeted inhibition of involved components.

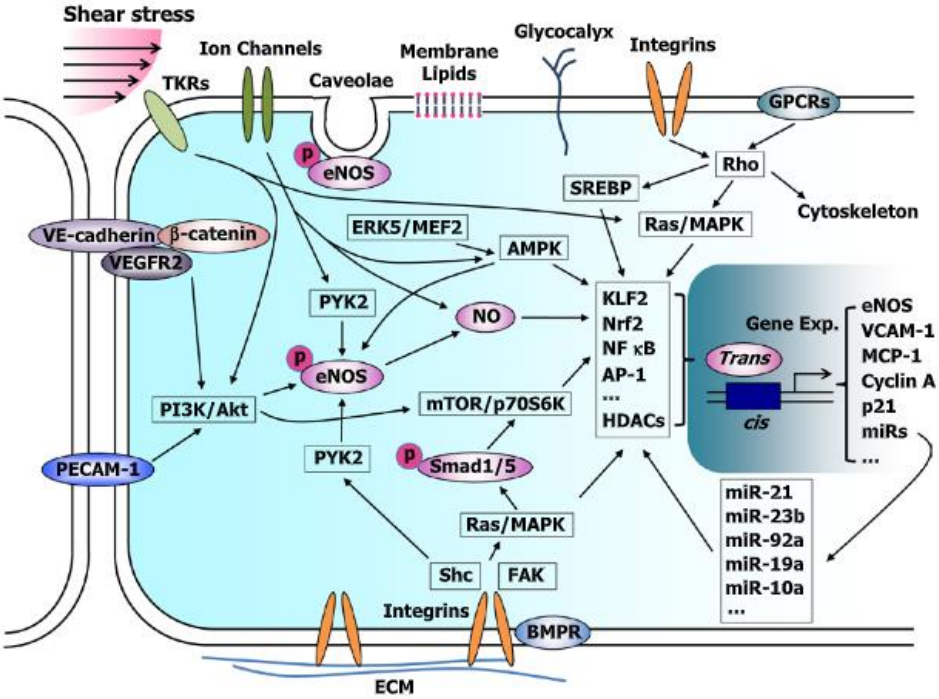

Figure 7: Schematic diagram illustrating the mechanobiological pathways of endothelial cells in response to shear stress. Shown mechanosensing components include integrins, PECAM -1, VE-cadherin, TKRs, ion channels, caveolae, membrane lipids, the glycocalyx and GPCRs, which start the signaling cascade of the remaining downstream effectors. Adapted from [8].

When little is known about the involved components in the underlying mechanism, a DNA microarray may be utilized to give a global overview of the expression profile [37, 46]. If more data about the underlying pathway is already available, a quantitative PCR (qPCR) might be better performed to analyze the expression levels of a smaller, more specific group of genes [22, 24, 45]. Then, through qPCR, the fold change can be computed, which tells if a gene is upregulated or downregulated (Figure 8A). If the involved components in the pathway are already known, enzyme-linked immunosorbent assays (ELISAs) can be performed, which utilize antibodies for the detection and quantification of specific antigens by a simple absorbance measurement [47]. Similarly, a western blot may be used to detect specific components of the pathway or, for example, investigate if the phosphorylation of a protein is involved. Additionally, the intensity (or width) of the band is directly proportional to the concentration of targeted protein (Figure 8B) [48, 49]. Alternatively, as described in previous sections, immunofluorescence could first be used for visualization, after which an image

analysis software can help determine the relative fluorescence intensity, which is occasionally used as a quantitative measure for the expression level [50]. Moreover, immunofluorescence also allows us to investigate whether, under a given condition, proteins localize more in the nucleus or in the cytoplasm by analyzing colocalization of different fluorescent labels (Figure 8C+D) [22, 24, 48].

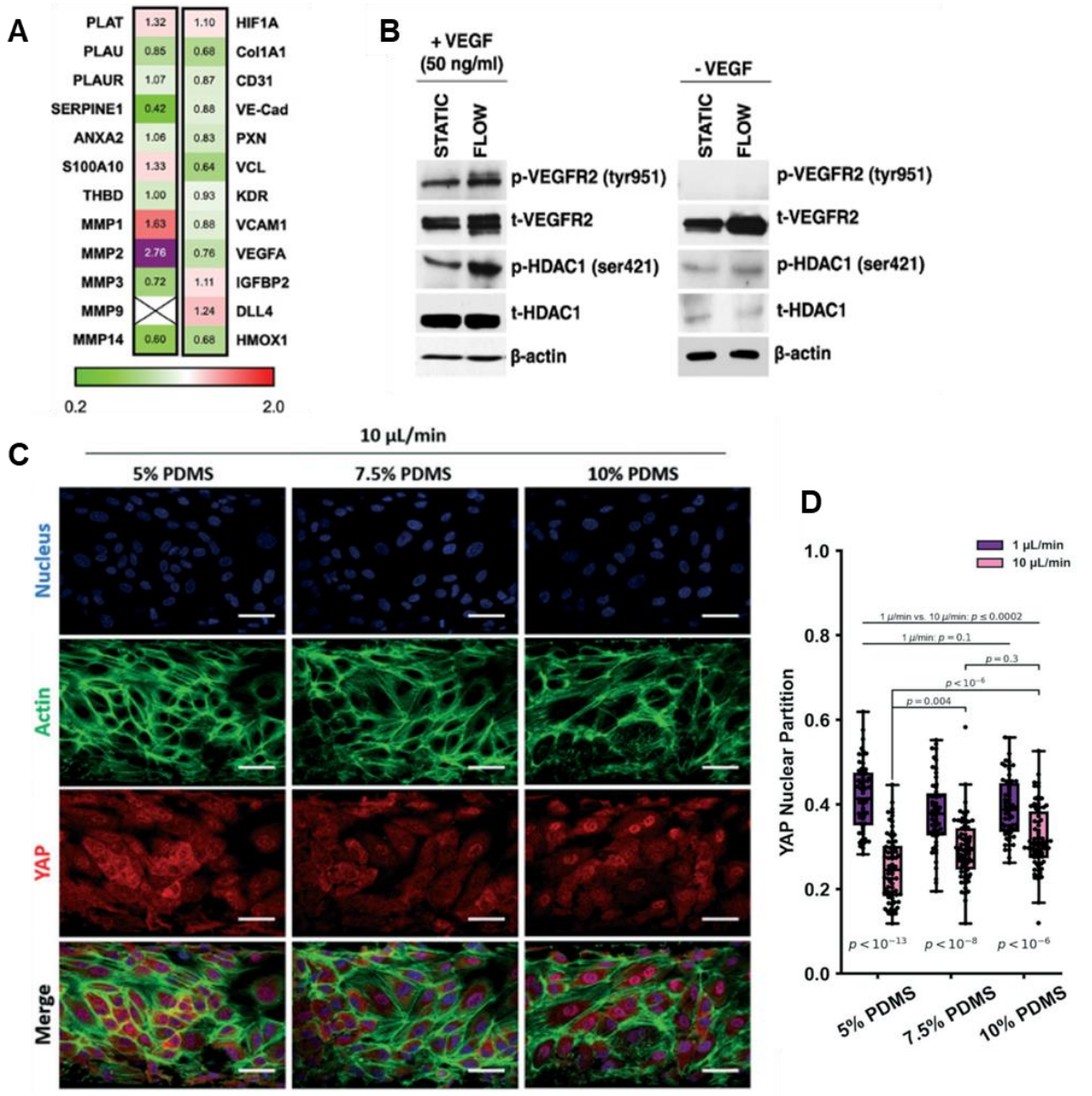

Figure 8: Characterization methods for investigating mechanobiological pathways. A) The fold change between HUVECs grown under static and interstitial flow conditions, evaluated by qPCR for various genes of interest, shows MMP2 is highly upregulated under interstitial flow. Adapted from [45]. B) Western blot demonstrates interstitial flow increases HDAC1 phosphorylation at Ser421 in HUVECs in response to VEGF; in presence of exogenous VEGF (50 ng/ml) p-HDAC1 has higher band intensity under flow, whereas in absence of exogenous VEGF there was no significant difference in p-HDAC1 band intensity between the static and flow condition. Adapted from [48]. C) HUVECs stained for nuclei (DAPI, blue), actin (phalloidin, green) and YAP (red) show increasing YAP nuclear localization with increasing substrate stiffness under 10 µL min^{-1}, which is quantified in D) with an image analysis software (cellSens, Olympus Corporation). C+D) Adapted from [22].

It is also possible that most of the involved components of a pathway have been identified, yet their exact role in the mechanism remains unclear. In this situation, different inhibition

methods can be used to target and block a component of interest, in order to determine its function. For example, function could be inhibited by enzymatic degradation of a component, for instance by degrading mechanosensing structures of the cell [26], or by RNA interference (RNAi), which effectively silences the expression of the target gene [48, 50], or lastly, by employing selective inhibitors, which directly affect the target protein's active site to prevent its function [45, 48]. Then, the previously discussed methods can again be used to evaluate the effect of inhibition on related gene expression levels and overall cell function. This process may then be repeated for other components until the characterization of the whole mechanobiological signaling system is eventually completed.

Table 2: Mechanobiological characterization in microfluidic endothelial models (2017-).

Cell type(s)	Stimulus analysed				Involved components (**mechano-sensing**, *downstream effector*)	Results	Ref.
	Shear Stress	**Flow types**	**Stiffness**	**Cyclic Strain**			
HUVECs	✓			✓	• eNOS	• Cyclic strain (10%); ↑ eNOS expression; ↑ NO production. • Cyclic strain (18%); also ↑ ROS released.	[25]
HUVECs	✓	✓	✓		• YAP, CTGF, ANKRD1	• High SS; ↓ CTGF expression. High SS + DF; ↑ ANKRD expression. Low SS or DF; ↑ CTGF expression. • Inhibition of YAP; ↓ CTGF expression but not ANKRD1. • High stiffness; ↑ YAP nuclear localization, any condition.	[22]
ECFCs HUAECs HUVECs hiPSC-ECs	✓				• **Primary cilia,** HDAC6**,** PLK-1	• SS (20 dyne/cm^2, 24h); progenitor + mature EC types align and elongate along flow direction in a cilia-dependent manner. • hiPSC-ECs; primary cilia assembly differs based on original cell line. Absence of cilia compromises mechanosensing. • Inhibition of HDAC6 rescues cilia formation and restores mechanosensing.	[37]
hASCs	✓				-	• SS range (7.8-13.7 dyne/cm^2) induces endothelial differentiation in hASCs.	[44]
HUVECS HLFs Brain ECs pericytes	✓	✓			• MMP-2	• IF; ↑ MMP-2 expression causing (↑ vessel density, ↑ diameter and ↑ perfusability) in fibrin gel. • Both in endothelial and brain microvascular model.	[45]

astrocytes							
hiPSC-ECs	✓				• **NOTCH1**, EphrinB2	• SS (≥ 3.8 dyne/cm^2, 40h); ↑ maturation into arterial phenotype with ↑ expression of NOTCH1, EphrinB2.	[43]
HAECs	✓				• **PECAM-1, ICAM-1**, p38, PI3K, ERK1/2, XBP-1	• SS is mechano-sensed by PECAM-1 and further signalled by PI3K; ↑ VCAM-1 and ICAM-1 expression. • Low SS, inhibition of p38 ↓ VCAM-1 expression. High SS; inhibition of ERK1/2 ↓ ICAM-1 expression. • SS; ↑ p38 phosphorylation; ↑ nuclear translocation of XBP-1; peak VCAM-1 expression. • ↑ VCAM-1 expression; ↑ monocyte adhesion.	[50]
UtMVECs, Endometrial stromal cells.	✓				• COX-2, cAMP.	• SS; activates ECs through COX-2, ↑ prostaglandin pathway. • Prostaglandins (PGI_2, PGE_2) sensitize endometrial stromal cells to P4, via cAMP pathway; ↑ decidualization.	[47]
HAVECs, VSMCs	✓			✓	• **NOTCH,** HEY1, Jag1	• SS; ECs + VSMCs align with flow. Cyclic strain; VSMCs align perpendicular. • Cell-cell contact; NOTCH signalling in ECs, HEY1 signalling in VSMCs.	[24]
HUVECs	✓	✓			• **VEGFR**, VEGF HDAC1**,** MMP14	• HDAC1 is key mechano-signalling component involved in angiogenesis. • IF + VEGF presence; ↑ HDAC1 phosphorylation + ↑ HDAC1 nuclear export. • HDAC-1; ↑ MMP14 expression.	[48]
HUVECs	✓	✓			-	• SS / BFF; ↓ EC permeability through NO-dependent mechanism. • SS / BFF + TVF; negates stabilizing effect of only SS/BFF to the static condition.	[30]
HUVECs	✓	✓			• Akt	• SS/BFF + DC-EF; ↑ EC permeability + ↓ VE-cadherin expression. • Inhibition of Akt negates the positive effects of DC-EF.	[51]
HUVECs	✓	✓			• **HSPG**	• High SS (15 dyne/cm^2); inhibits neovascularization + stabilizes EC layer. • Regulated by HPSG mechanosensing.	[52]

HEKCs	✓				• **Piezo1, α5β1, αvβ3 and αvβ5 integrins**	• Piezo1 mechanosensitivity is regulated by ECM composition: • High SS (10 dyne/cm²); fibronectin ↑ mechanosensitivity through α5β1 + αvβ3 integrins. • Low SS (2 dyne/cm²); collagen (type I, IV) + laminin ↑ mechanosensitivity through αvβ3 + αvβ5 integrins.	[53]

Abbreviations:

Stimuli:
Shear stress (SS), disturbed flow (DF), interstitial flow (IF), transvascular flow (TVF), bifurcated fluid flow (BFF), direct current-electric field (DC-EF).

Cells types:
Endothelial cells (ECs), uterine microvascular ECs (UtMVECs), human lung fibroblasts (HLF), human umbilical vein ECs (HUVECs), human induced pluripotent stem cell derived-ECs. (hiPSC-ECs), Endothelial colony-forming cells (ECFCs), human umbilical arterial ECs (HUAECs), human aortic ECs (HAECs), human aortic vein EC (HAVECs), vascular smooth muscle cells (VSMCs), human carotid artery ECs (HCAECs), Human adipose-derived stem cells (hASCs),

Molecules:
Matrix metalloproteinase-2 (MMP-2), cyclooxygenase-2 (COX-2), cyclic adenosine monophosphate (cAMP), prostacyclin (PGI2), prostaglandin E2 (PGE2), progesterone (P4), yes-associated protein (YAP), connective tissue growth factor (CTGF), ankyrin repeat domain 1 (ANKRD1), histone deacetylase 6 (HDAC6), polo-like kinase 1 (PLK-1), histone deacetylase 6 (HDAC1), matrix metalloproteinase-14 (MMP14), vascular endothelial growth factor (VEGF), platelet EC adhesion molecule-1 (PECAM-1), intercellular adhesion molecule-1 (ICAM-1), x-box protein-1 (XBP-1), phosphoinositide 3-kinase (PI3K), extracellular signal-regulated kinases-1/2 (ERK1/2), nitric oxide (NO), protein-kinase B (Akt), endothelial nitric oxide synthase (eNOS), reactive oxygen species (ROS), heparan sulfate proteoglycan (HSPG).

5. Discussion

Currently, a considerable portion of the published literature is still focused on the development of new microfluidic endothelial models and their validation. As a result, many types of models exist that serve the same purpose. For example, in this review, a large number of the reviewed studies that focused on characterizing the effects of flow also utilized their own unique microfluidic endothelial model [10, 17, 21, 22, 25, 31, 35, 36, 44, 48, 51, 54]. This raises the question which models are most effective but also how this could be determined, since at the moment there is no standardized framework in place for the validation of a new model and evaluation of its functionality. As a result, like discussed in section 2 & 3, each study selects its own parameters to validate their new model, which complicates comparison between models. Therefore, in order to advance the field, it would make sense that a framework is established, which should include standards for validation of mechanical stimuli (*e.g.* a minimal accuracy of computational flow models) and of observed biological effects (*e.g.* comparable permeability to normal vessel structure, maximum range of stress fiber orientation), so models can be effectively compared before investigating mechanobiological effects. Then, the development of new models can mostly focus on addressing current problems or adding new features that, for example, allow for easier characterization.

Commonly discussed problems in characterization are mostly associated with the quantification methods of the mechanobiology pathways, which were discussed in the last section. There, the small scale of microfluidic devices can actually be disadvantageous, because the low number of cells results in low protein contents that may be too low to accurately measure [48, 50]. Another contributing factor, can be a faster degradation rate in response to trypsinization, which makes the measured gene expression dependent on the half-life of its mRNA and the analysis time [22]. While there are methods to work around these obstacles when performing characterization, such as upscaling the model [48] to larger millifluidic systems and simply working faster, it is not as straightforward. In the future, more research in the field of non-destructive analyses can help to address some of these problems, including the requirement of higher cellular content in the models.

Additionally, the models could be improved by increasing their complexity with additional features. For characterization specifically, this may mean the incorporation of sensors [25] or open designs that allow for advanced imaging [31] combined with automated image analysis systems [18]. However, it is more likely to first see an increase in model complexity with respect to the use of various EC types and combinations of different cell types in cocultures. As we saw in section 4, HUVECs are currently the most used cell type, however, in the future it could be of interest to start comparing the behavior of a wider range of EC types and cell lines. This is relevant because the mechanosensing ability of hiPSC-ECs was reported to vary depending on their original cell line [37]. Furthermore, the use of more different cell types in cocultures is also an important step to make in the future towards more physiologically-relevant models. Lastly, the integration of multiple mechanical stimuli in the model would be interesting for future work. Including those not discussed in this review, such as different topographies or ECM composition. For example, it would be interesting to investigate the mechanobiological response to mechanical stimuli under different ECM compositions, as different integrins were already shown to be activated depending on ECM composition [53].

Overall, there is still a lot to gain concerning microfluidic endothelial models in the future. While as time passes, a shift from model development and validation towards more

investigation is expected, there will always be room for more development. As other fields advance, better characterization procedures can be applied, and the new models can incorporate state-of-the art technologies for mechanobiology assessment. Step-by-step, the models should aim to become more biomimetic and the characterization methods more effective, which could lead to new discoveries in fundamental mechanobiology.

6. References

1. Charbonier, F.W., M. Zamani, and N.A.-O. Huang, *Endothelial Cell Mechanotransduction in the Dynamic Vascular Environment.* (2366-7478 (Print)).
2. Kwak, B.R., et al., *Biomechanical factors in atherosclerosis: mechanisms and clinical implications.* (1522-9645 (Electronic)).
3. Nagelkerke, A., et al., *The mechanical microenvironment in cancer: How physics affects tumours.* Seminars in Cancer Biology, 2015. **35**: p. 62-70.
4. H. Ritchie, F., Spooner, M. Roser, *Causes of death.* Our World in Data, 2018(https://ourworldindata.org/causes-of-death).
5. Duval, K., et al., *Modeling Physiological Events in 2D vs. 3D Cell Culture.* (1548-9221 (Electronic)).
6. Gray, K.M. and K.M. Stroka, *Vascular endothelial cell mechanosensing: New insights gained from biomimetic microfluidic models.* Seminars in Cell & Developmental Biology, 2017. **71**: p. 106-117.
7. Popele, N.M.v., et al., *Association Between Arterial Stiffness and Atherosclerosis.* Stroke, 2001. **32**(2): p. 454-460.
8. Zhou, J., Y.S. Li, and S. Chien, *Shear stress-initiated signaling and its regulation of endothelial function.* (1524-4636 (Electronic)).
9. Huang, G., et al., *Engineering three-dimensional cell mechanical microenvironment with hydrogels.* Biofabrication, 2012. **4**(4): p. 042001.
10. Yu, H., et al., *A Microfluidic Model Artery for Studying the Mechanobiology of Endothelial Cells.* Advanced Healthcare Materials, 2021. **10**(18): p. 2100508.
11. Ziółkowska, K., R. Kwapiszewski, and Z. Brzózka, *Microfluidic devices as tools for mimicking the in vivo environment.* New Journal of Chemistry, 2011. **35**(5): p. 979.
12. Polacheck, W.J., et al., *Microfluidic platforms for mechanobiology.* Lab on a Chip, 2013. **13**(12): p. 2252.
13. Xue, C., et al., *Substrate stiffness regulates arterial-venous differentiation of endothelial progenitor cells via the Ras/Mek pathway.* Biochimica et Biophysica Acta (BBA) - Molecular Cell Research, 2017. **1864**(10): p. 1799-1808.
14. Low, W.S., N.A. Kadri, and W.A.B.b. Wan Abas, *Computational Fluid Dynamics Modelling of Microfluidic Channel for Dielectrophoretic BioMEMS Application.* The Scientific World Journal, 2014. **2014**: p. 961301.
15. Gad-el-Hak, M., *Liquids: The holy grail of microfluidic modeling.* Physics of Fluids, 2005. **17**(10): p. 100612.
16. Bruus, H., *Chapter 1 Governing Equations in Microfluidics*, in *Microscale Acoustofluidics*. 2015, The Royal Society of Chemistry. p. 1-28.
17. Mei, X., et al., *Microfluidic platform for studying osteocyte mechanoregulation of breast cancer bone metastasis.* Integrative Biology, 2019. **11**(4): p. 119-129.
18. Sonmez, U.M., et al., *Endothelial cell polarization and orientation to flow in a novel microfluidic multimodal shear stress generator.* Lab on a Chip, 2020. **20**(23): p. 4373-4390.
19. Venugopal Menon, N., et al., *A tunable microfluidic 3D stenosis model to study leukocyte-endothelial interactions in atherosclerosis.* APL Bioengineering, 2018. **2**(1): p. 016103.
20. Middleton, K., et al., *Microfluidics approach to investigate the role of dynamic similitude in osteocyte mechanobiology.* Journal of Orthopaedic Research, 2018. **36**(2): p. 663-671.

21. Pérez-Rodríguez, S., et al., *Microfluidic model of monocyte extravasation reveals the role of hemodynamics and subendothelial matrix mechanics in regulating endothelial integrity.* Biomicrofluidics, 2021. **15**(5): p. 054102.
22. Walther, B.K., et al., *Mechanotransduction-on-chip: vessel-chip model of endothelial YAP mechanobiology reveals matrix stiffness impedes shear response.* Lab on a Chip, 2021. **21**(9): p. 1738-1751.
23. Luo, Q., et al., *Cell stiffness determined by atomic force microscopy and its correlation with cell motility.* Biochimica et Biophysica Acta (BBA) - General Subjects, 2016. **1860**(9): p. 1953-1960.
24. van Engeland, N.C.A., et al., *A biomimetic microfluidic model to study signalling between endothelial and vascular smooth muscle cells under hemodynamic conditions.* Lab on a Chip, 2018. **18**(11): p. 1607-1620.
25. Jin, Z.-H., et al., *Integrating Flexible Electrochemical Sensor into Microfluidic Chip for Simulating and Monitoring Vascular Mechanotransduction.* Small, 2020. **16**(9): p. 1903204.
26. Inglebert, M., et al., *The effect of shear stress reduction on endothelial cells: A microfluidic study of the actin cytoskeleton.* Biomicrofluidics, 2020. **14**(2): p. 024115.
27. Claesson-Welsh, L., *Vascular permeability--the essentials.* (2000-1967 (Electronic)).
28. Cai, A., C. Chatziantoniou, and A. Calmont, *Vascular Permeability: Regulation Pathways and Role in Kidney Diseases.* Nephron, 2021. **145**(3): p. 297-310.
29. Díaz-Montes, E. *Dextran: Sources, Structures, and Properties*. Polysaccharides, 2021. **2**, 554-565 DOI: 10.3390/polysaccharides2030033.
30. Akbari, E., et al., *Flow dynamics control endothelial permeability in a microfluidic vessel bifurcation model.* Lab on a Chip, 2018. **18**(7): p. 1084-1093.
31. Salman, M.M., et al., *Design and Validation of a Human Brain Endothelial Microvessel-on-a-Chip Open Microfluidic Model Enabling Advanced Optical Imaging.* Frontiers in Bioengineering and Biotechnology, 2020. **8**.
32. Boussommier-Calleja, A., et al., *The effects of monocytes on tumor cell extravasation in a 3D vascularized microfluidic model.* (1878-5905 (Electronic)).
33. Levesque Mj Fau - Nerem, R.M. and R.M. Nerem, *The elongation and orientation of cultured endothelial cells in response to shear stress.* (0148-0731 (Print)).
34. Katoh, K., S. Kano Y Fau - Ookawara, and S. Ookawara, *Role of stress fibers and focal adhesions as a mediator for mechano-signal transduction in endothelial cells in situ.* (1178-2048 (Electronic)).
35. Tovar-Lopez, F., et al., *A Microfluidic System for Studying the Effects of Disturbed Flow on Endothelial Cells.* Frontiers in Bioengineering and Biotechnology, 2019. **7**.
36. Mohammed, M., et al., *Studying the Response of Aortic Endothelial Cells under Pulsatile Flow Using a Compact Microfluidic System.* Analytical Chemistry, 2019. **91**(18): p. 12077-12084.
37. Smith, Q., et al., *Differential HDAC6 Activity Modulates Ciliogenesis and Subsequent Mechanosensing of Endothelial Cells Derived from Pluripotent Stem Cells.* Cell Reports, 2018. **24**(4): p. 895-908.e6.
38. *Chapter 33 - Actin and Actin-Binding Proteins*, in *Cell Biology (Third Edition)*, T.D. Pollard, et al., Editors. 2017, Elsevier. p. 575-591.
39. abcam. *Phalloidin staining protocol*. 2021; Available from: https://www.abcam.com/protocols/phalloidin-staining-protocol.
40. Tkachenko, E., et al., *The nucleus of endothelial cell as a sensor of blood flow direction.* (2046-6390 (Print)).

41. Dejgaard, S.Y., K. Dejgaard, and J.F. Presley, *Cell Staining: Fluorescent Labelling of the Golgi Apparatus*, in *eLS*. 2010.
42. Kocherova, I.A.-O., et al., *Human Umbilical Vein Endothelial Cells (HUVECs) Co-Culture with Osteogenic Cells: From Molecular Communication to Engineering Prevascularised Bone Grafts. LID - 10.3390/jcm8101602 [doi] LID - 1602.* (2077-0383 (Print)).
43. Arora, S., et al., *Determination of critical shear stress for maturation of human pluripotent stem cell-derived endothelial cells towards an arterial subtype.* Biotechnology and Bioengineering, 2019. **116**(5): p. 1164-1175.
44. Kim, H.W., et al., *Investigation of effective shear stress on endothelial differentiation of human adipose-derived stem cells with microfluidic screening device.* Microelectronic Engineering, 2017. **174**: p. 24-27.
45. Zhang, S., et al., *Interstitial Flow Promotes the Formation of Functional Microvascular Networks In Vitro through Upregulation of Matrix Metalloproteinase-2.* Advanced Functional Materials. **n/a**(n/a): p. 2206767.
46. Yee, A.J. and S. Ramaswamy, *Chapter 7 - DNA Microarrays in Biological Discovery and Patient Care*, in *Essentials of Genomic and Personalized Medicine*, G.S. Ginsburg and H.F. Willard, Editors. 2010, Academic Press: San Diego. p. 73-88.
47. Gnecco, J.S., et al., *Hemodynamic forces enhance decidualization via endothelial-derived prostaglandin E2 and prostacyclin in a microfluidic model of the human endometrium.* Human Reproduction, 2019. **34**(4): p. 702-714.
48. Bazou, D., et al., *Flow-induced HDAC1 phosphorylation and nuclear export in angiogenic sprouting.* Scientific Reports, 2016. **6**(1): p. 34046.
49. Pillai-Kastoori, L., A.R. Schutz-Geschwender, and J.A. Harford, *A systematic approach to quantitative Western blot analysis.* Analytical Biochemistry, 2020. **593**: p. 113608.
50. Bailey, K.A., et al., *Mechanoregulation of p38 activity enhances endoplasmic reticulum stress-mediated inflammation by arterial endothelium.* The FASEB Journal, 2019. **33**(11): p. 12888-12899.
51. Mohana Sundaram, P., et al., *Direct current electric field regulates endothelial permeability under physiologically relevant fluid forces in a microfluidic vessel bifurcation model.* Lab on a Chip, 2021. **21**(2): p. 319-330.
52. Zhao, P., et al., *Flow shear stress controls the initiation of neovascularization via heparan sulfate proteoglycans within a biomimetic microfluidic model.* Lab on a Chip, 2021. **21**(2): p. 421-434.
53. Lai, A., et al., *Piezo1 Response to Shear Stress Is Controlled by the Components of the Extracellular Matrix.* ACS Applied Materials & Interfaces, 2022. **14**(36): p. 40559-40568.
54. Concilia, G., et al., *Investigating the mechanotransduction of transient shear stress mediated by Piezo1 ion channel using a 3D printed dynamic gravity pump.* Lab on a Chip, 2022. **22**(2): p. 262-271.